Proposal for considering the group effect in the prediction of settlements in pile groups through load transfer methods

Francisco Vladson Cardins Gomes Filho[1#] (ID), Alfran Sampaio Moura[1] (ID)

Article

Abstract
When designing a foundation project, it is necessary to ensure that all the elements meet both ultimate and serviceability limit states, which call for predictions of settlement and load capacity. The load transfer methods are a widely used alternative to estimate the load-settlement ratio of piles in the design of foundation projects. However, traditional load transfer methods do not consider the interactive effects between the elements in pile groups. This study proposes changes to the load transfer curves developed by Bohn et al. (2016), aiming to incorporate the group effect in the analysis of load-settlement relationships in pile groups. Comparisons between the predicted settlements obtained using the proposed method and the results of load tests performed by Dai et al. (2012) in Jiangsu, China, showed that the modifications proposed in this study agreed well with the experimental results for most of the analyzed groups.

1. Introduction

Settlement prediction is an important task that can be performed using different techniques, such as the load transfer methods, which use load transfer functions (called "t-z" and "q-z" curves) to determine the load-settlement relationship for a pile. These load transfer curves can be developed from theoretical solutions and empirical observations.

Load transfer functions were used to describe relationship between unit skin friction and pile settlement and the relationship between the pile tip resistance and the pile tip displacements. Some examples of this application are present in Zhang & Zhang (2012a, b), Wang et al. (2012) and Lee et al. (2013).

Nowadays most multi-storey buildings use pile groups. Thus, in order to determine the settlements, the interactive effects between them (i.e., group effect) should be considered. However, most of the current methods to estimate settlements analyze the piles separately, without considering the influence of the neighboring ones on the field behavior of the pile group.

Bohn et al. (2016) used the load transfer curves to predict settlement in isolated piles. This study analyzed several load transfer curves, comparing the curves to the results collected in the field. Fellenius (2018) discussed the analyses made by Bohn et al. (2016) and it was concluded that, among the several functions analyzed in the study, the

hyperbolic load transfer curves obtained good agreement to the measured results.

The present study aims to propose changes to the load transfer functions for single piles proposed by Bohn et al. (2016) in order to incorporate the group effect in the analysis of load-settlement ratios of pile groups.

2. Development of a t-z load transfer function to predict settlement in pile groups

The hyperbolic t-z load transfer function proposed by Bohn et al. (2016) to calculate the settlement of a single pile can be expressed as shown in Equation 1.

$$\tau_s = \frac{\tau_{s,ult} s_{si}}{M_s D + s_{si}} \tag{1}$$

where τ_s is the mobilized skin friction; $\tau_{s,ult}$ is the ultimate unit resistance; s_{si} is the displacement of the analyzed element (the single pile); D is the pile diameter; and M_s is the deformation parameter, which can be obtained from Bohn et al. (2016).

In order to consider the group effect in the function, the term s_{si} can be isolated, as shown in Equation 2.

#Corresponding author. E-mail address: vladson@alu.ufc.br
[1]Universidade Federal do Ceará, Departamento de Engenharia Hidráulica e Ambiental, Fortaleza, CE, Brasil.

$$s_{si} = \frac{\tau_s M_s D}{\left(\tau_{s,ult} - \tau_s\right)} \qquad (2)$$

Following the procedure suggested by Zhang et al. (2010, 2016), Zhang & Zhang (2012a) and Pan et al. (2018), the term related to the displacement, which is induced by the stress q_s from the neighboring piles, is added to Equation 2. In sequence, the additional settlement is calculated according to the formulations proposed by Randolph & Wroth (1979) and Mylonakis & Gazetas (1998), as shown in Equations 3 and 4.

$$\Delta S_s = \zeta_s \tau_s \qquad (3)$$

where ΔS_s is the increase in displacement caused by the group effect; ζ_s is the interaction factor; and τ_s is the mobilized lateral resistance.

$$\zeta_s = \sum_{j \neq 1, j=1}^{n} \frac{r_0}{G_s} \ln\left(\frac{2.5l(1-\upsilon)}{r_{ij}}\right) - \sum_{j \neq i, j=1}^{n} \frac{r_0^2}{G_s r_{ij}} \ln\left(\frac{2.5l(1-\upsilon)}{r_{ij}}\right) \qquad (4)$$

where r_0 is the radius of analyzed pile; G_S is the shear modulus of the soil layer where the analyzed element is located; l is the pile length; υ is the Poisson's ratio of the soil layer where the analyzed element is located; and r_{ij} is the distance between axes (centers) of two considered piles.

The total displacement of the shaft that is caused by the applied loads on the analyzed pile plus the neighboring ones can thus be written as in Equation 5, where the additional portion of settlement caused by the group effect is added.

$$s_s = \frac{\tau_s M_s D}{\left(\tau_{s,ult} - q_s\right)} + \zeta_s \tau_s \qquad (5)$$

Equation 5 can be rewritten as shown in Equation 6.

$$\tau_s = \frac{\left(M_s D + \tau_{s,ult}\zeta_s + s_s\right) - \sqrt{\left(M_s D + \tau_{s,ult}\zeta_s + s_s\right)^2 - 4\left(-\zeta_s\right)\left(-s_s \tau_{s,ult}\right)}}{2\zeta_s} \qquad (6)$$

And Equation 6 can be simplified by defining the terms a_{gs} and b_{gs} as in Equations 7 and 8.

$$a_{gs} = M_s D + \tau_{s,ult}\zeta_s \qquad (7)$$

$$b_{gs} = -4\zeta_s \tau_{s,ult} \qquad (8)$$

By substituting the values of a_{gs} and b_{gs}, Equation 6 can be rewritten as Equation 9, thus obtaining the expression for the modified t-z load transfer function.

$$\tau_s = \frac{\left(a_{gs} + s_s\right) - \sqrt{\left(a_{gs} + s_s\right)^2 + b_{gs}s_s}}{2\zeta_s} \qquad (9)$$

The development described above was implemented by Zhang et al. (2010) for load transfer curves of single piles. The present study implemented a similar procedure but modifying the load transfer functions proposed by Bohn et al. (2016), which were developed based upon a greater number of load tests when compared to Zhang et al. (2010) and also considered load tests carried out in Brazilian soils.

3. Development of a q-z load transfer function to predict settlement in pile groups

The hyperbolic q-z load transfer function developed by Bohn et al. (2016) to calculate settlement of single piles can be written as Equation 10.

$$q_b = \frac{q_{b,ult}s_{bi}}{M_b D + s_{bi}} \qquad (10)$$

The term s_{bi} can be isolated, in a similar procedure to that used for the t-z curve, as shown in Equation 11.

$$s_{bi} = \frac{q_b M_b D}{\left(q_{b,ult} - q_b\right)} \qquad (11)$$

The additional settlement was calculated according to the formulations proposed by Randolph & Wroth (1979) and can be seen in Equations 12 and 13. The variable q_b is the mobilized resistance, $q_{b,ult}$ is the ultimate resistance, s_{bi} is the pile toe displacement, and M_b is the toe deformation parameter. Values for M_b can be obtained from Bohn et al. (2016).

$$\Delta S_b = \zeta_b q_b \qquad (12)$$

$$\zeta_b = \sum_{j=1, j \neq i}^{n} \frac{1 - v_b}{2\pi G_b r_{ij}} \qquad (13)$$

The pile tip displacement due to the loading on top of both analyzed pile and neighboring piles can then be expressed as shown in Equation 14.

$$s_b = \frac{q_b M_b D}{\left(q_{b,ult} - q_b\right)} + q_b \zeta_b \qquad (14)$$

Isolating the term q_b, the obtained solution (Equation 15) corresponds to the modified q-z load transfer function, with the terms a_{gb} and b_{gb} being defined respectively as in Equations 16 and 17.

$$q_b = \frac{\left(a_{gb} + s_b\right) - \sqrt{\left(a_{gb} + s_b\right)^2 + b_{gb}s_b}}{2\zeta_b} \qquad (15)$$

$$a_{gb} = M_b D + q_{b,ult}\zeta_b \qquad (16)$$

$$b_{gb} = -4\zeta_b q_{b,ult} \tag{17}$$

Thus, from the expressions proposed in Equations 9 and 15, the group effect can be considered in the prediction of settlements in pile groups.

4. Analyzed case - Dai et al. (2012)

The experimental data used as input in this study were extracted from Dai et al. (2012) and comprised load tests performed on 32 bored piles (single and groups of 2, 4, and 9 piles), in an experimental field located in Jiangsu, China. Table 1 presents a summary with the characteristics of single piles and pile groups.

The compressive strength of the concrete used in pile shafts and caps was 25 MPa, with a Young's Modulus of 29.2 GPa, obtained from compression tests performed in 6 prismatic specimens (100 mm × 100 mm × 300 mm), tested 28 days after casting. According to Bohn et al. (2016), the pile caps could be considered as rigid.

A hole called BH was drilled down to a depth of 29.50 m, aiming to obtain soil samples and the surrounding stratigraphy. In addition, 4 cone penetration tests were carried out (CPT1, CPT2, CPT3, and CPT4). A layout of the experimental field displaying the location of piles, drilled hole BH (stratigraphy), and performed CPTs can be found in Dai et al. (2012).

The stratigraphy showed layers of clay and silt in the upper depths. A layer of soft clay was also identified between the depths of 17.0 m and 29.50 m and water level was located at 2.6 m below ground surface.

The load tests were performed until pile failure. The reaction system consisted of prismatic blocks of precast concrete and a platform supported by 12 m-long reaction piles, installed 5 m away from the center of tested groups. The maximum load applied was 1.2 times the estimated load capacity for each group.

4.1 Method

In order to obtain the load-settlement ratios for the pile groups analyzed by Dai et al. (2012), the modified t-z and q-z curves (Equations 9 and 15) were used. The pile shafts were subdivided into 1 m-long segments, each one of them corresponding to a t-z curve, determined according to the properties of the soil layer in which the segment was located. This same discretization was adopted by Zhang et al. (2016) and Pan et al. (2018).

Values for M_s were obtained based on the chart presented by Bohn et al. (2016) and Poisson's ratio was assumed as 0.45, according to Dai et al. (2012). Table 2 presents the values for the ultimate unitary resistance ($q_{s,ult}$) and M_s per section of the 20-m-long piles (i.e. groups QZ2, QZ4, and QZ9).

Table 1. Characteristics of piles studied by Dai et al. (2012).

Identification	Number of piles	Length (m)	Spacing
DZ1	1	20.0	-
DZ1L	1	24.0	-
QZ2	2	20.0	2.5D
QZ2L	2	24.0	3.0D
QZ4	4	20.0	2.5D
QZ4L	4	24.0	3.0D
QZ9	9	20.0	2.5D
QZ9L	9	24.0	3.0D

Table 2. Values for $q_{s,ult}$ and M_s for the 20 m-long pile groups.

Section (m)	Soil type	Measured $q_{s,ult}$ (kPa)	M_s
0-1	Clay	30.7	0.00280
1-2	Clay	29.6	0.00280
2-3	Clay	52.4	0.00280
3-4	Clay	86.6	0.00280
4-5	Clay and Silt	77.8	0.00300
5-6	Silt	64.8	0.00330
6-7	Silt	64.8	0.00330
7-8	Silt	64.8	0.00330
8-9	Silt	64.8	0.00330
9-10	Silt	64.8	0.00330
10-11	Silt and silty-sand	62.9	0.00330
11-12	Silt and silty-sand	62.5	0.00330
12-13	Silt and silty-sand	62.5	0.00330
13-14	Silt and silty-sand	62.5	0.00330
14-15	Silt and silty-sand	62.5	0.00330
15-16	Silt and silty-sand	62.5	0.00330
16-17	Silt and silty-sand	62.5	0.00330
17-18	Silt, silty-sand and soft clay	44.0	0.00305
18-19	Soft clay	25.5	0.00280
19-20	Soft clay	25.5	0.00280

In this method, the values for ultimate unitary lateral resistances for pile groups – the input parameters – were those regarding single piles, as presented in Table 2. Thus, the values for ultimate unitary lateral resistances obtained for pile DZ1 were used for the 20 m-long pile groups, and the values for pile DZ1L, for the 24 m-long ones.

The t-z and q-z curves for single piles were converted into pile group curves by considering the interactive effects between piles (group effect), according to the development

described in Sections 2 and 3 of this study. Table 3 shows the values for ultimate unitary resistance and M_s per section for groups QZ2L, QZ4L, and QZ9L (24 m-long piles).

For both 20 m- and 24 m-long piles, the adopted M_b was 0.0088. The load capacity obtained by Dai et al. (2012) for the single pile DZ1 (20 m) was 1,430 kN and for the single pile DZ1L (24 m), 1,540 kN. Both values were obtained through load tests.

Most of the applied load was absorbed by the shaft. The toe resistance mobilized in failure was 4.73 kN for DZ1 and 78.54 kN for DZ1L. These were the values used in q-z load transfer functions.

In the approach here described, the load-settlement relationships of the piles were obtained through an interactive procedure, similar to that proposed by Coyle & Reese (1966), Zhang & Zhang (2012a) and Zhang et al. (2016).

1. [Step 1] The pile is subdivided into n segments. A displacement S_b is chosen for the pile toe (segment n). From this displacement and using the q-z curve (Equation 15), the mobilized load P_b at pile tip is calculated, multiplying toe stress q_b by the tip area.

Table 3. Values for $q_{s,ult}$ and M_s for the 24 m-long pile groups.

Section (m)	Soil type	Measured $q_{s,ult}$ (kPa)	M_s
0-1	Clay	32.35	0.0028
1-2	Clay	32.10	0.0028
2-3	Clay	54.90	0.0028
3-4	Clay	89.10	0.0028
4-5	Clay and silt	78.30	0.0030
5-6	Silt	62.10	0.0033
6-7	Silt	62.10	0.0033
7-8	Silt	62.10	0.0033
8-9	Silt	62.10	0.0033
9-10	Silt	62.10	0.0033
10-11	Silt and silty-sand	59.78	0.0033
11-12	Silt and silty-sand	59.20	0.0033
12-13	Silt and silty-sand	59.20	0.0033
13-14	Silt and silty-sand	59.20	0.0033
14-15	Silt and silty-sand	59.20	0.0033
15-16	Silt and silty-sand	59.20	0.0033
16-17	Silt and silty-sand	59.20	0.0033
17-18	Silt, silty-sand and soft clay	40.80	0.00305
18-19	Soft clay	22.40	0.0028
19-20	Soft clay	22.40	0.0028
20-21	Soft clay	22.40	0.0028
21-22	Soft clay	22.40	0.0028
22-23	Soft clay	22.40	0.0028
23-24	Soft clay	22.40	0.0028

2. [Step 2] The displacement of the midpoint of analyzed segment (S_s) is estimated. For the first iteration, $S_s = S_b$.
3. [Step 3] Using the t-z curve (Equation 9) and the displacement S_s, the shear stress q_s mobilized in the lateral area of analyzed segment can be calculated.
4. [Step 4] The force due to friction (ΔP_n) acting on the side of analyzed segment is calculated (Equation 18):

$$\Delta P_n = \tau_s \pi L_i \tag{18}$$

where L_i is the length of analyzed segment; and τ_s is shear stress mobilized in the shaft of analyzed segment.

5. [Step 5] The force acting at the top of analyzed segment (P_{tn}) is determined according to Equation 19.

$$P_{tn} = P_b + \Delta P_n \tag{19}$$

6. [Step 6] The elastic shortening of the lower half of analyzed segment is calculated according to Equation 21, using the axial force which acts at the midpoint of analyzed segment ($P_{n,med}$) and the force acting at its base (P_b).

$$P_{n,med} = \frac{P_{tn} + P_b}{2} \tag{20}$$

$$\Delta e / 2 = \frac{P_{nmed} + P_b}{2} \frac{(\Delta L_n / 2)}{E_p A_p} \tag{21}$$

where ΔL_n is the variation in the length of analyzed element; E_p is Young's Modulus of the pile; and A_p is pile cross-sectional area.

7. [Step 7] A new displacement for the midpoint of analyzed segment (S_s') is calculated, adding the elastic shortening ($\Delta e/2$) to the displacement of the base of segment S_b, according to Equation 22.

$$S_s' = S_b + \Delta e / 2 \tag{22}$$

8. [Step 8] The value of S_s' is compared with S_s. If they differ by more than 10^{-6} m, the procedure from steps 2 to 7 is repeated, assuming S_s' as the new value for S_s, until the convergence for analyzed segment is reached.
9. [Step 9] After the convergence is reached, the displacement at the top of analyzed segment (S_{tn}) is calculated, according to Equation 23.

$$S_{tn} = S_b + \Delta e \tag{23}$$

10. [Step 10] The displacement of the top of analyzed segment corresponds to the displacement of the base of the upper segment. Therefore, the procedure is repeated, until load and settlement are obtained for the top segment of pile.

The procedure described above is replicated for several values of S_b until the load-settlement ratio for the range of loads of interest is obtained.

Equations 9 and 15 require the soil shear modulus of each soil layer to be applied, which in this case was estimated for each stress level. For this purpose, the soil shear wave velocity (V_s) was determined using Equation 24 for granular soil layers, proposed by Baldi et al. (1989) and Equation 25 for fine soil layers, proposed by Mayne (1995), which correlate CPT's penetration resistance with V_s.

$$V_s = 277 q_c^{0.13} \sigma_{vo}^{'\ 0.27} \qquad (24)$$

$$V_s = 1.75 q_c^{0.627} \qquad (25)$$

where σ'_{vo} is the effective geostatic stress of soil in the center of analyzed layer.

From the shear wave values for each layer, the maximum shear modulus (G_{max}) can be calculated, according to Equation 26.

$$G_{max} = \frac{\gamma_n}{g} V_s^2 \qquad (26)$$

where g is the acceleration of gravity; and γ_n is the soil unit weight.

From G_{max}, the shear modulus (G) is obtained for each analyzed load, using another iterative procedure, as described below (Steps A to E). This geotechnical parameter is obtained using Equations 24 and 25, for each layer, considering the thickness of each layer.

11. [Step A] A load at the top of pile (P_t') is estimated. From the load capacity of the single pile, a factor of safety (FS) is determined.
12. [Step B] Using Equation 27 (Fahey & Carter, 1993), the shear modulus (G_s) of each layer can be also determined.

$$\frac{G_s}{G_{máx}} = 1 - \left(\frac{1}{FS}\right)^{0.3} \qquad (27)$$

13. [Step C] The iterative procedure described in Steps A and B is performed again, using the calculated values for G. Then, a new load P_t is obtained.
14. [Step D] The obtained P_t is compared with the estimated P_t. If the obtained value is smaller than the estimated one, a larger displacement S_b is used in the beginning of the procedure. If the obtained P_t is greater, a smaller S_b displacement should be used.
15. [Step E] The procedure is repeated until the difference between the estimated P_t' and the obtained P_t is not greater than 0.1 kN.

5. Results of predictions and analyses

5.1 Analyzed case study – Dai et al. (2012)

The case study described by Dai et al. (2012) was used in this study to evaluate the modified t-z and q-z curves and the proposed methodology. At the end of this section, some possible causes for differences between the predicted (calculated) and measured results will be presented.

Figure 1 shows both the predicted and the experimental (obtained by Dai et al., 2012) load-settlement curves for groups QZ2 (2 piles) and QZ2L (2 piles). The method proposed in this study yielded results that agreed quite well with the experimental ones, especially for loads up to 2,500 kN. For higher loads, the predicted settlements were slightly higher than those experimentally measured.

Considering a factor of safety (FS) of 2.0 (i.e. an adopted workload of 1,250 kN), a difference of only 1.5 mm (absolute value) was observed between the predicted and the experimentally measured settlements.

As to group QZ2L, the predicted settlements also agreed well with the experimental results for loads up to 1,500 kN. The predicted results were closest to those measured for the load of 1,100 kN. Between 1,500 kN and 2,800 kN, the predicted (calculated) results were slightly lower than those obtained experimentally. Above 2,800 kN, the method yielded higher values for settlement than those obtained experimentally.

Figure 2 shows the predicted and the experimental (Dai et al., 2012) load-settlement curves for groups QZ4 (4 piles, 20-m-long piles) and QZ4L (4 piles, 24-m-long piles). Good agreement was observed between predicted and experimental results up to 1,500 kN. For higher loads, the predicted settlements were smaller than those obtained experimentally. These were the most discordant results (between experimental and predicted) considering all analyzed groups, which might have happened due to differences in stiffness of the soils around the single piles and the pile groups.

Regarding group QZ4L, predicted results were remarkably close to experimental ones, notably for loads below 1,500 kN. Between 1,500 kN and 2,800 kN, experimental results were slightly higher than estimated ones. For load levels above 2,800 kN, the method provided settlements also slightly higher than those experimentally obtained.

Figure 3 shows the load-settlement curves for pile groups QZ9 and QZ9L. For group QZ9, excellent agreement between predicted and experimental results was obtained, especially for loads under 7,500 kN. For higher loads, the predicted results were slightly lower than those experimentally obtained. One of the possible causes for the divergence may be a reduced soil stiffness in the area of installation of this group, in comparison to the area of installation of isolated piles.
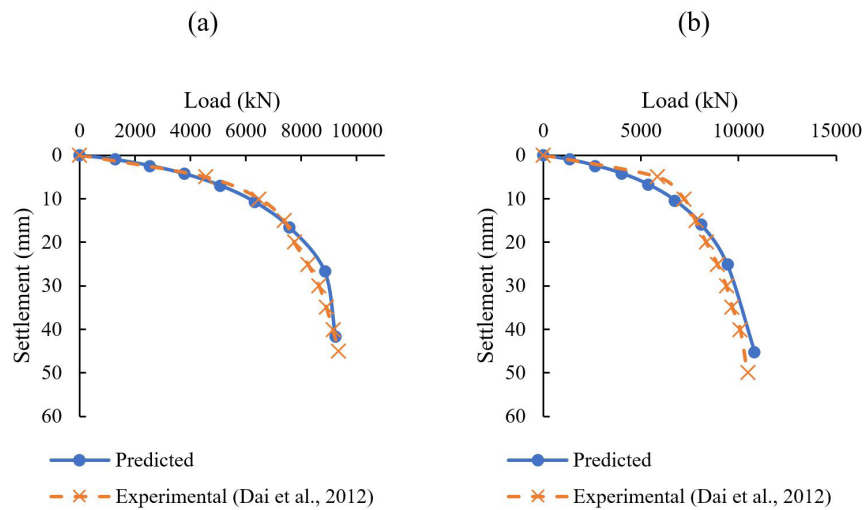
For group QZ9L, predicted and experimental results agreed as well. The most consistent results were for loads between 0 and 3,000 kN. Around 6,000 kN, the predicted settlements were slightly higher than the experimental ones.

(a)

(b)
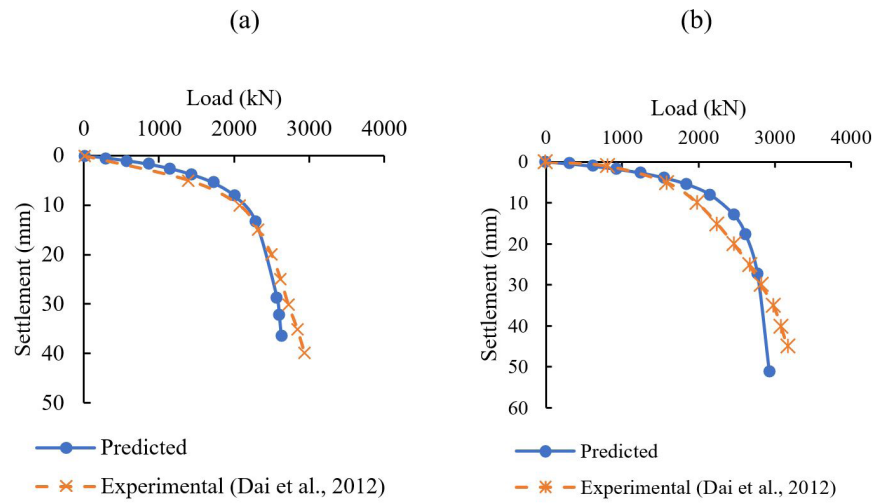
Figure 1. Predicted and experimental load-settlement curves for (a) group QZ2 and (b) group QZ2L.

(a)

(b)
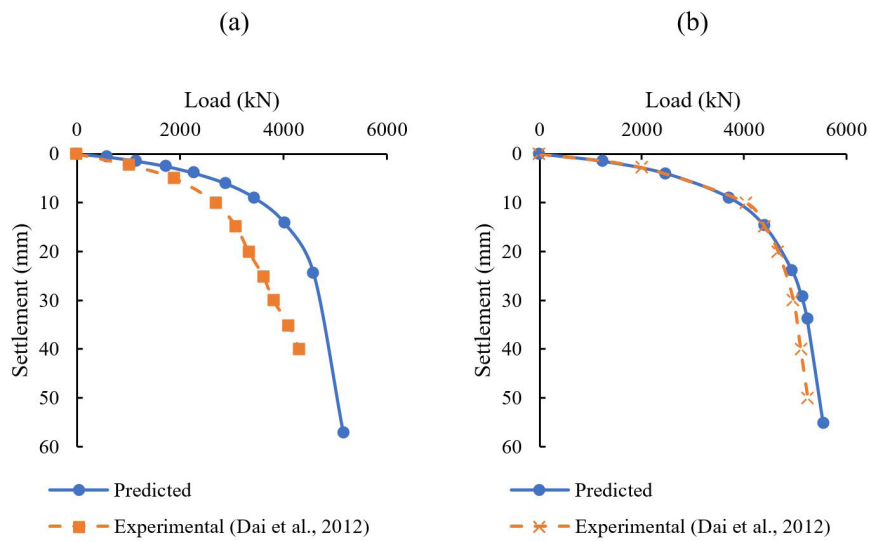
Figure 2. Predicted and experimental load-settlement curves for (a) group QZ4 and (b) group QZ4L.

(a)

(b)

Figure 3. Predicted and experimental load-settlement curves for (a) group QZ9 and (b) group QZ9L.

For loads above 8,000 kN, the experimental results were slightly higher than those predicted.

In general, the method proposed in this study yielded settlements that reasonably agreed with experimental results, notably for groups QZ4L and QZ9. However, some divergences between experimental and predicted results were still observed, particularly for group QZ4.

These small divergences probably happened due to soil heterogeneity, for CPT results showed that soil stiffness was not the same in all assessed locations. Thus, as the used input parameters came both from load tests and CPTs carried out on single piles, it is possible that the stiffness in the regions where the load tests were performed was different from where CPTs were performed.

Another possible reason for the differences in the results reside in the choice for the parameters M_s, M_b, and shear modulus. Although estimated considering the results of 72 load tests, more accurate values for M_s and M_b could have been obtained if a greater number of load tests had been used for each pile and soil types.

As to shear modulus, although the correlations were calibrated considering a large amount of data and showed good adherence to them, it is possible that the values could be a little distant from field reality, which could also be a possible cause for the divergences between predicted and experimental settlements.

6. Conclusions

The present work proposed modifications to the t-z and q-z curves developed by Bohn et al. (2016), in order to consider the group effect in the analysis of load-settlement ratios in pile groups. The modifications were carried out using the interaction factors proposed by Randolph & Wroth (1979) and Mylonakis & Gazetas (1998).

Regarding groups QZ2 and QZ2L, the method proposed in this study yielded results with good agreement with experimental ones, especially for loads up to 2,500 kN. For loads above 2,500 kN, the predicted settlements were slightly higher than those experimentally measured.

For the group QZ4, good agreement was also observed between predicted and experimental results, mainly for loads up to 1,500 kN.

For the group QZ4L, predicted results were quite close to experimental ones, notably for loads below 750 kN. For load levels above 1,400 kN, the predicted settlements were slightly higher than those experimentally obtained.

Regarding groups QZ9 and QZ9L, good agreement between predicted and experimental results was also obtained, especially for loads under 7,500 kN. For higher loads, the predicted results were slightly lower than experimental ones. The geotechnical parameter G_{max} were obtained by correlations with CPT.

Thus, the predictions for load-settlement ratios made according to the modifications proposed in this study for t-z and q-z curves agreed quite well with the experimental data for most analyzed pile groups, even though considerable divergences between experimental and predicted settlements were also obtained (block QZ4), most likely due to soil heterogeneity, evidenced by results from cone penetration tests (CPTs).

Declaration of interest

The authors declare no conflict of interest in this research.

Author's contributions

Francisco Vladson Cardins Gomes Filho: data curation, formal analysis, investigation, methodology, software, visualization, validation, writing – original draft, writing – review & editing. Alfran Sampaio Moura: conceptualization, project administration, supervision, validation, writing – review & editing.

List of symbols

τ_s	Mobilized unit lateral resistance
$\tau_{s,ult}$	Ultimate unit lateral resistance
D	Pile diameter
M_s	Deformation parameter for t-z curve
s_{si}	Displacement of the analyzed element
ζ_s	Lateral interaction factor
ΔS_s	Increase in displacement of the analyzed element caused by the group effect
r_0	Radius of pile
G_S	Shear modulus of soil layer where the element is located
υ	Poisson's ratio of soil layer where the element is located
r_{ij}	Distance between axes (centers) of two considered piles
q_b	Mobilized unit base resistance
$q_{b,ult}$	Ultimate unit base resistance
s_{bi}	Base displacement
M_b	Deformation parameter for q-z curve
ΔS_s	Increase in base displacement caused by the group effect
ζ_b	Base interaction factor
G_b	Shear modulus of the base soil layer
υ_s	Poisson's ratio of the base soil layer
ΔP_n	Force due to friction

L_i	Length of analyzed segment
P_{tn}	Force acting at the top of analyzed element
P_b	Force acting at the base of analyzed element
$P_{n,med}$	Axial force which acts at the midpoint of analyzed segment
ΔL_n	Variation in the length of analyzed element
Δe	Elastic shortening
S_s'	Displacement of the midpoint of analyzed segment
S_{tn}	Displacement at the top of analyzed segment
V_s	Soil shear wave velocity
q_c	Cone penetration resistance
G_{max}	Maximum soil shear modulus
g	Acceleration of gravity
γ_n	Soil unit weight
FS	Safety factor

References

Baldi, G., Bellotti, R., Gionna, V.N., Jamiolkowski, M., & Lo Presti, D.C.F. (1989). Modulus of sands from CPT's and DMT's. In *Proceedings of the 12th International Conference on Soil Mechanics and Foundation Engineering* (Vol. 1, pp. 1-6), Rio de Janeiro. Publications Committee of XII ICSMFE.

Bohn, C., Santos, A.L., & Frank, R. (2016). Development of axial pile load transfer curves based on instrumented load tests. *Journal of Geotechnical and Geoenvironmental Engineering*, 143, 2-6. http://dx.doi.org/10.1061/(ASCE)GT.1943-5606.0001579.

Coyle, H.M., & Reese, L.C. (1966). Load transfer for axially loaded piles in clay. *Journal of the Soil Mechanics and Foundations Division*, 92(2), 1-26. http://dx.doi.org/10.1061/JSFEAQ.0000850.

Dai, G., Salgado, R., Gong, W., & Zhang, Y. (2012). Load tests on full-scale bored pile groups. *Canadian Geotechnical Journal*, 49(11), 1293-1308. http://dx.doi.org/10.1139/t2012-087.

Fahey, M., & Carter, J.P. (1993). A finite element study of the pressuremeter test in sand using nonlinear elastic plastic model. *Canadian Geotechnical Journal*, 30(2), 348-362. http://dx.doi.org/10.1139/t93-029.

Fellenius, B.H. (2018). Discussion of "development of axial pile load transfer curves based on instrumented load tests". *Journal of Geotechnical and Geoenvironmental Engineering*, 144(4), 07018005. http://dx.doi.org/10.1061/(ASCE)GT.1943-5606.0001867.

Lee, J., You, K., Jeong, S., & Kim, J. (2013). Proposed point bearing load transfer function in jointed rock-socketed drilled shafts. *Soil and Foundation*, 53(4), 596-606. http://dx.doi.org/10.1016/j.sandf.2013.06.010.

Mayne, P.W. (1995). *Evaluation of foundation response by G/G_{max} degradation relationships in soils* (pp. 136-148). Taipei: National Science Council of ROC and NSF of U.S.

Mylonakis, G., & Gazetas, G. (1998). Settlement and additional internal forces of grouped piles in layered soil. *Geotechnique*, 48(1), 55-72. http://dx.doi.org/10.1680/geot.1998.48.1.55.

Pan, D.D., Zhang, Q.Q., Liu, S.W., & Zhang, M.S. (2018). Analysis on response of a single pile and pile groups based on the Runge-Kutta method. *KSCE Journal of Civil Engineering*, 22(1), 92-100. http://dx.doi.org/10.1007/s12205-017-0578-x.

Randolph, M.F., & Wroth, C.P. (1979). An analysis of the vertical deformation of pile groups. *Geotechnique*, 29(4), 423-439. http://dx.doi.org/10.1680/geot.1979.29.4.423.

Wang, Z.J., Xie, X.Y., & Wang, J.J.C. (2012). A new nonlinear method for vertical settlement prediction of a single pile and pile groups in layered soils. *Computers and Geotechnics*, 45(9), 118-126. http://dx.doi.org/10.1016/j.compgeo.2012.05.011.

Zhang, Q.Q., Zhang, Z.M., & He, J.Y. (2010). A simplified approach for settlement analysis of single pile and pile groups considering interaction between identical piles in multilayered soils. *Computers and Geotechnics*, 37(7-8), 969-976. http://dx.doi.org/10.1016/j.compgeo.2010.08.003.

Zhang, Q.Q., & Zhang, Z.M. (2012a). A simplified nonlinear approach for single pile settlement analysis. *Canadian Geotechnical Journal*, 49(11), 11256-11266. http://dx.doi.org/10.1139/t11-110.

Zhang, Q.Q., & Zhang, Z.M. (2012b). Simplified calculation approach for settlement of single pile and pile groups. *Journal of Computing in Civil Engineering*, 26(6), 750-758. http://dx.doi.org/10.1061/(ASCE)CP.1943-5487.0000167.

Zhang, Q.Q., Liu, S.W., Zhang, S.M., Zhang, J., & Wang, K. (2016). Simplified non-linear approaches for response of a single pile and pile groups considering progressive deformation of pile-soil system. *Soil and Foundation*, 56(3), 473-484. http://dx.doi.org/10.1016/j.sandf.2016.04.013.